applied sciences

MDPI

Article

Joint Resource Allocation and Learning Optimization for UAV-Assisted Federated Learning

Chaoyi Liu [1,2] and Qi Zhu [1,2,*]

[1] Jiangsu Key Laboratory of Wireless Communications, Nanjing University of Posts and Telecommunications, Nanjing 210003, China
[2] Engineering Research Center of Health Service System Based on Ubiquitous Wireless Networks, Nanjing University of Posts and Telecommunications, Ministry of Education, Nanjing 210003, China
* Correspondence: zhuqi@njupt.edu.cn

Abstract: Aiming at the unmanned aerial vehicle (UAV)-assisted federated learning wireless-network scenario, and considering the influence of the UAV altitude on the coverage area, we propose a joint optimization algorithm of UAV placement, computation and communication resources. Considering the energy efficiency and federated learning performance, we defined the cost function of the system. Under the constraint of the total delay of federated learning completion, we formulated an optimization problem of minimizing the cost function to achieve the balance between the total energy consumption of users and the federated learning performance. Since the formulated optimization problem is a non-convex problem, in order to solve this problem, we decomposed it into three optimization subproblems: UAV horizontal placement, local accuracy and computation and communication resources. We used successive convex approximation (SCA), the Dinkelbach Method, the Bisection method and KKT condition, respectively, to solve the three subproblems, and finally obtain the optimal solutions through iteration of the three subproblems. Simulation results show that compared with the federated learning scenario under fixed UAV altitude, our proposed algorithm not only guarantees the learning performance, but also reduces more users' total energy consumption.

Keywords: machine learning; energy efficiency; learning performance; Dinkelbach method

check for updates

Citation: Liu, C.; Zhu, Q. Joint Resource Allocation and Learning Optimization for UAV-Assisted Federated Learning. *Appl. Sci.* **2023**, *13*, 3771. https://doi.org/10.3390/app13063771

Academic Editor: Christos Bouras

Received: 2 February 2023
Revised: 8 March 2023
Accepted: 12 March 2023
Published: 15 March 2023

Copyright: © 2023 by the authors. Licensee MDPI, Basel, Switzerland. This article is an open access article distributed under the terms and conditions of the Creative Commons Attribution (CC BY) license (https://creativecommons.org/licenses/by/4.0/).

1. Introduction

In recent years, with the popularity of smart devices and the continuous expansion of the Internet of Things' scale, a quantity of the data show an exponentially increasing trend [1]. Through the analysis and processing of these data, some intelligent applications (face recognition, intelligent driving, voice recognition) have been developed rapidly, but at the same time, it also raises the issue of data security and privacy. In addition, as people gradually pay more attention to privacy issues, more and more entities begin to emphasize the attribution and use rights of data, reducing the data exchange between different entities, making each entity gradually become an "isolated data island" [2]. So as to solve the above problems, give greater play to the value of data and improve the performance of artificial intelligence algorithms, scholars have put forward a new paradigm, Federated Learning (FL), which has the ability to crack the "isolated data island" problem and protect privacy. Federated learning was first proposed by H. Bradley McMahan et al. [3], as it can coordinate the joint learning of all parties without exposing the data of all parties. Compared with traditional centralized learning, it not only improves the utilization rate of wireless resources, but also guarantees the privacy of users. In the process of FL, participants do not need to upload local original data, they only need to upload data-related neural network model parameters, and then the master server security aggregates model parameters, and provides feedback to participants. Then, participants according to their own dataset update the global model, effectively ensuring the security and privacy of each

participant's sensitive data. Although FL can effectively solve the problems of the "isolated data island" and privacy, it also faces great challenges: the participant problem and the communication problem. In the FL process, as more participants have increased data diversity, the learning ability of the trained model will be stronger. Moreover, the model parameters need to be exchanged frequently among all parties, and the central party often needs to wait for all user's training models to be uploaded before it can conduct security aggregation or other data processing. For example, in case of user drop off or communication block, etc. The central party will be trapped in the infinite waiting process, which seriously affects the efficiency of model aggregation and FL.

Therefore, the current research focuses of FL are how to establish a perfect incentive and selection mechanism, encourage more participants to join, select participants with high quality data, how to propose a way to ensure the FL efficiency and how to improve the quality and capacity of communication channels. On the one hand, the participant problems of FL over wireless networks have been studied in [4–9]. In [4], Nishio T et al. investigated user scheduling algorithms that maximize the number of participating users in each global round to improve FL test performance. Motivated by [4], Yoshida N et al. [5] proposed a client scheduling scheme based on the multi-armed bandit (MAB) theory, which balanced the selection of clients with uncertain resources and known large resources. In addition, Xu B et al. [6] proposed an online client scheduling scheme based on the greedy algorithm, which reduces the number of training rounds and the time interval of each global round. Based on age of update (AOU) measurements, Yang H. H et al. [7] proposed a scheduling strategy, which jointly considers the stability of received parameters and instantaneous channel quality to improve FL operation efficiency. In addition, Ren J et al. [8] investigated the gradient average effect over participating clients in each global round, and proposed a scheduling strategy to select high-quality clients by taking into account the diversity of channels and the "importance" of clients' updates. An FL task-training model based on contract theory was proposed in [9], which minimized the incentive budget according to the individual rationality (IR) and incentive compatibility (IC) of users in each FL training round. However, the authors of [4–9] only started from the perspective of how to select and motivate users, and did not consider the optimization of the clients' energy consumption. When too many clients participate, as the number of wireless resources is fixed, the clients' energy consumption will rise sharply, which is unfavorable to clients with limited energy storage. Moreover, if users suddenly quit the learning process, it will also have an impact on learning performance. On the other hand, the communication problems of FL over wireless networks have been investigated in [10–13]. In [10], Yang Z et al. researched the computation and communication resource allocation of FL on wireless networks, and under the condition that constraints are met, an iterative algorithm was proposed to derive the closed-form solutions of transmission time, transmission bandwidth, transmission power, computation frequency and local accuracy. Luo S et al. [11] introduced a Hierarchical Federated Edge Learning (HFEL) framework in which model aggregation was partially migrated from the cloud to the edge server, and formulated a joint wireless resource allocation and user edge association problem to minimize the energy and latency. Zeng Q et al. [12] proposed a new computation and communication resource framework, which uses multiple processors of clients to simultaneously process data, and jointly controls bandwidth allocation, CPU-GPU workload allocation, computation frequency of processors and transmission time. In addition, the study in [12] was further extended by Ruby R et al. [13], within a certain time budget, solving the problem of resource allocation in the HFEL structure. However, in [10–13] the authors were only concerned with the optimization of the client energy without setting a suitable client scheduling scheme. When the number of users reaches a critical value, the data owned by the users may contain all the data features of the overall dataset. Therefore, the FL learning performance will not be significantly improved with the increase in the user numbers. In addition, some users' data quality may be very poor, and if this user participates, the FL learning performance will be degraded.

In summary, in [4–13] the proposals have only considered the participant or communication problem in FL unilaterally, without comprehensively thinking about the effect of user choice and terminal energy consumption in FL. So, in the work of [14], Thi Le et al. put forward an auction game as an incentive mechanism between the base station (BS) and users, with each user submitting bids based on the minimal energy consumption to participate in FL, and a primal–dual greedy auction mechanism was introduced to determine the winners and maximize social welfare. In the case that the uplink transmission may be wrong, Chen M et al. [15] formulated the optimization problem of minimizing FL loss function and proposed an optimization scheme of wireless resource allocation and user selection. Under the framework of HFEL, Wen W et al. [16] introduced a user selection and resource allocation strategy to take into account the uncertainty of wireless channels and the importance of the weighted gradient. Moreover, in the case of users' data that are independently identically distributed (IID) and non-IID, Liu S et al. [17] studied the optimization problem by optimizing user association and resource allocation. In [18], Shi W et al. proposed a jointly optimized user selection and resource allocation strategy to maximize the FL test accuracy within a given total FL completion time. In particular, based on a novel technique, namely over-the-air computation, Yang K et al. [19] investigated client scheduling and beam-forming design in FL. In addition, Al-Abiad M. S et al. [20] studied the optimization problem of multi-layer FL under non-orthogonal multiple access (NOMA), and proposed a resource allocation scheme with the total energy consumption of Internet of Things' devices as the optimization objective. Moreover, Xiao H et al. [21] studied FL in the scenario of the Internet of Vehicles, considering the position and speed of vehicles, and a minimum–maximum optimization problem was formulated to optimize the computation frequency, communication power and local accuracy to achieve the minimum cost.

As an aerial mobile-base station, UAVs can quickly build a wireless network and provide emergency communication services. It plays an important role in earthquakes, floods, fire and other emergencies as well as battlefield operations. Due to their mobility, compared with fixed base stations, UAVs can find a suitable location to reduce the transmission energy consumption of users. Therefore, with the purpose of further improve the FL performance, UAVs can be combined with FL. Tursunboev, J et al. [22] proposed a novel and high-performing FL scheme to improve FL performance. By considering the unavailability of ground BS and the limited energy of users, Pham Q. –V et al. [23] deployed a UAV equipped with edge computation and wireless power communications (WPC) capabilities to perform FL missions, and proposed an algorithm that jointly optimize the UAV's position, local accuracy and wireless resources to minimize the energy consumption of UAVs and users. Based on the premise that UAV-assisted users upload models, Ng J. S et al. [24] established the coalition formation game to maximize the sum of UAV individual profit, according to users' preferences over heterogeneous UAVs, and proposed a joint auction–coalition to achieve a stable partition of the UAV coalitions and applied an auction scheme to solve the allocation of the UAV coalition. Under the limitation of learning accuracy and training delay, Jing Y et al. [25] proposed a jointly optimized UAV placement and resource allocation to reduce the energy consumption of use. In addition, based on reinforcement learning, Yang H et al. [26] proposed an asynchronous federated learning (AFL) framework, which implemented asynchronous distributed computation, and proposed an asynchronous advantage actor–critic (A3C) reinforcement learning algorithm by joint optimizing device selection, UAVs' position and resource allocation to improve the FL convergence speed and test accuracy. However, in [23–26], the altitude of the UAV is fixed. In fact, the UAV's coverage area should be related to the UAV's altitude. The higher the hover position of the UAV, the greater the chance of air-to-ground line of sight transmission, that is, the larger the coverage radius, which means the larger the service range of the UAV and more users can access, the faster the FL converges. However, the higher the deployment height, the larger the signal transmission distance will be, resulting in greater path loss and increased energy consumption of users participating in FL. Therefore, the height deployment of UAVs needs to be optimized. Based on the above analysis, in the UAV-assisted

federated learning wireless scenario, this paper takes into account the impact of the UAV's height on the coverage area, and under the constraint of completing the total delay, realizes the balanced optimization of users' total energy consumption and FL performance through the joint optimization of the UAV's position (height, horizontal position), local accuracy and computation and communication resources. The main contributions of this paper are summarized as follows.

(1) For the UAV-assisted federated learning wireless network scenario, by considering the impact of the UAV's altitude on coverage area, we defined the system's cost function which is composed of the total energy consumption and the reciprocal of the participating user number, and formulated a cost function minimization–optimization problem within a given total FL completion time budget. By jointly optimizing the UAV's position (horizontal placement, altitude), computation frequency, communication power, communication bandwidth, communication time and local accuracy this can realize the balanced optimization between the user's total energy consumption and FL performance;

(2) Because the formulated problem is not convex, we decomposed it into three optimization subproblems: UAV horizontal placement, local accuracy and user computation and communication resources. For subproblem 1 (UAV horizontal placement), firstly we introduced a relaxation variable, and then used the first order Taylor expansion to transform it into a convex problem. Finally, we used successive convex approximation (SCA) to obtain the optimal UAV placement;

(3) For subproblem 2 (local accuracy), since it is a fractional form, first of all we converted the fractional form into the integral form, and then used the Dinkelbach method to obtain the optimal local accuracy; For subproblem 3 (computation and communication resources), this paper further decomposed it into two sub-problems, namely, transmission power, computation frequency, transmission time optimization subproblem 3-1 and transmission bandwidth optimization subproblem 3-2. For subproblem 3-1, it was deduced that the optimal solution of transmission time can be acquired by using the bisection method, furthermore, the optimal solution of transmission power and computation frequency is obtained. For subproblem 3-2, since this problem is convex, the optimal solution can be obtained by using the KKT condition.

The rest of this paper is organized as follows: Section 2 shows the system model and problem formulation. Section 3 presents the joint optimization algorithm. Section 4 analyzes the simulation results and performance analysis. Conclusions are drawn in Section 5. For convenience, the key notations used in this paper are summarized in Table 1.

Table 1. Key Notations.

Symbol	Definitions	Symbol	Definitions
n, m	index of the user, UAV	κ	effective switched capacitance
N	total number of users	g_n	channel gain of user n
$\mathcal{N}$	set of users	f_n	CPU frequency of user n
$\mathcal{N}_m$	set of within the UAV m service range	C_n	number of CPU cycles for user n to computing one sample data
N_m	user number within the UAV m service range	b_n	transmission bandwidth of user n
$\mathcal{D}_n$	training dataset of user n	p_n	transmission power of user n
D_n	training dataset size of user n	η	local accuracy

Table 1. *Cont.*

Symbol	Definitions	Symbol	Definitions
$\mathbf{x}_{nk}$	k-th input data of user n	ε_0	global accuracy
$\mathbf{w}$	neural network model parameters	N_0	noise power spectral density
s	neural network model $\mathbf{w}$ size	$p^{\max}$	maximum transmission power
h, θ	UAV altitude, UAV angle	$f^{\max}$	maximum calculated frequency
$\mathbf{q}_m = \{x_m, y_m\}$	UAV m horizontal placement	T	the completion time of FL
$\mathbf{q}_n = \{x_n, y_n\}$	user n placement	B	total bandwidth
r	coverage radius of the UAV	ρ	weight coefficient
I_l, I_g	local training rounds, global rounds	L, γ, ξ	parameter associated with the loss function

2. System Model and Problem Formulation

As shown in Figure 1, we consider an FL wireless network that consists of UAV m and N users, denoted as a set by $\mathcal{N} = \{1, 2 \dots N\}$. The users of the UAV service range are represented by set $\mathcal{N}_m$, with N_m users. As the central party of FL, the UAV first initializes a global model, and then sends it to users within its service range. After receiving the model, the users update it according to the local dataset, and upload the updated model to the UAV, which then aggregates the local model weighted.

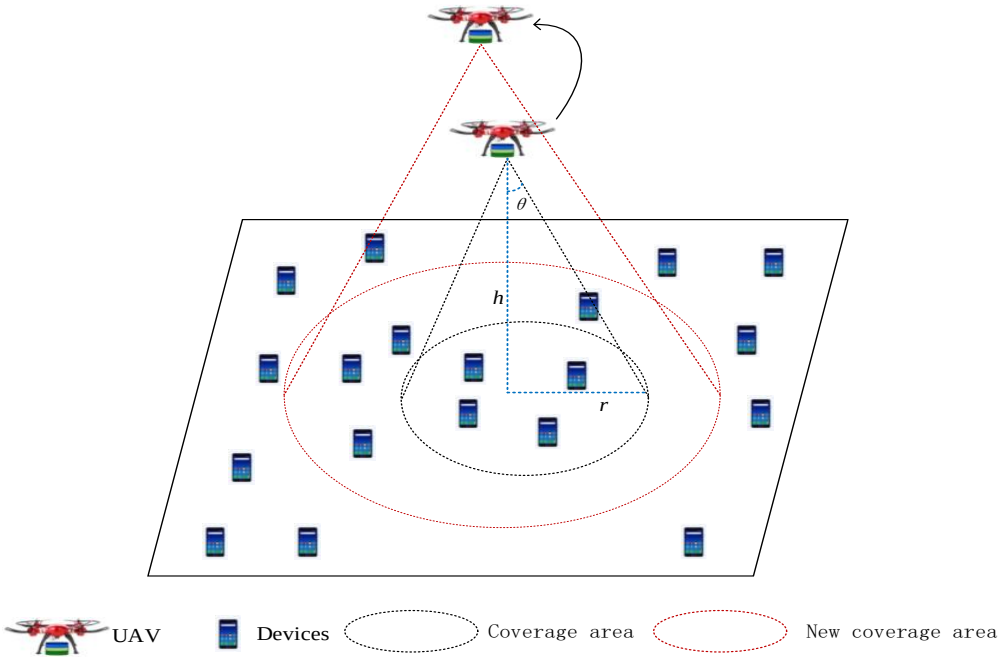


Figure 1. System model.

Each user n has a dataset $\mathcal{D}_n$, with D_n data samples. For dataset $\mathcal{D}_n = \{\mathbf{x}_{nk}, y_{nk}\}_{k=1}^{D_n}$, $\mathbf{x}_{nk} \in \mathbb{R}^d$ is an k-th input data of user n and y_{nk} is its corresponding label. According to the local dataset $\mathcal{D}_n$, the user n updates the FL model, and the loss function of user n is

$$f_n(\mathbf{w}) = \frac{1}{D_n} \sum_{k \in \mathcal{D}_n} f(\mathbf{w}, \mathbf{x}_{nk}, y_{nk}), \forall n \in \mathcal{N}_m \tag{1}$$

where $\mathbf{w}$ denotes the neural network model parameters; and the loss function $f(\mathbf{w}, \mathbf{x}_{nk}, y_{nk})$ measures neural network model parameters $\mathbf{w}$ on user n k-th sample models differ degree.

Meanwhile, for different FL tasks, the neural network defines a different loss function; usually mean square error or cross entropy is used as the loss function.

After user n completes the model training and updates according to the local dataset, it is uploaded to the UAV. The UAV m aggregates the collected local model, and its aggregate model and loss function are

$$\mathbf{w} = \sum_{i \in \mathcal{N}_m}^{|\mathcal{N}_m|} \frac{D_i}{D_m} \mathbf{w}_i \tag{2}$$

$$F(\mathbf{w}) = \sum_{i \in \mathcal{N}_m}^{|\mathcal{N}_m|} \frac{D_i}{D_m} f_i(\mathbf{w}) \tag{3}$$

where $D_m = \sum_{i \in \mathcal{N}_m}^{|\mathcal{N}_m|} D_i$ represents the total data amount of users participating in FL within the service range of the UAV m.

The goal of FL is to constantly repeat the user local model update and to transmit it to the UAV for aggregation to minimize $F(\mathbf{w})$, and finally obtain $\mathbf{w}$ that satisfies the demand. That is

$$\min_{\mathbf{w}} F(\mathbf{w}) = \min_{\mathbf{w}} \sum_{i \in \mathcal{N}_m}^{|\mathcal{N}_m|} \frac{D_i}{D_m} f_i(\mathbf{w}) \tag{4}$$

In order to solve (4), the DANE algorithm was used to solve the problem. The specific process details have been shown in [10], so we will not elaborate too much here.

2.1. Network Model

The UAV's hover altitude is h and angle is θ, θ is the effective illumination angle of the UAV, so the coverage radius of the UAV is $r = h\tan(\theta)$. Assume that all users within the coverage radius participate in FL training. The horizontal placement of the UAV m and user n are represented as $\mathbf{q}_m = \{x_m, y_m\}$ and $\mathbf{q}_n = \{x_n, y_n\}$, respectively. The distance between the UAV m and user n is $d_{nm} = \sqrt{h^2 + \|\mathbf{q}_m - \mathbf{q}_n\|_2^2}$, therefore, the channel gain of user n is $g_n = g_0 \left(\frac{d_{nm}}{d_0}\right)^{-\alpha}$, where g_0 represents the channel power gain at d_0 is 1 meter (m), the value is same as that in [27].

2.2. Computing and Communication Model

The energy consumption of users directly affects the user experience. Therefore, this paper focuses on the energy consumption of users in the FL process, including the training and communication energy consumption.

2.2.1. Computation Model

The training delay of user n in one iteration of FL is

$$T_n^{comp} = \frac{I_l C_n D_n}{f_n}, \ \forall n \in \mathcal{N}_m \tag{5}$$

where D_n is the data volume of user n and f_n denotes the CPU frequency of user n, which is measured by the number of CPU cycles per second; C_n is the number of CPU cycles required for computing one sample data at user n; and I_l is the local training rounds for each global round at user n.

According to [10], when the required local accuracy reaches η, the I_l needs to satisfy the condition: $I_l \geq \frac{2}{(2-L\delta)\delta\gamma} \log\left(\frac{1}{\eta}\right)$, so $I_l = \frac{2}{(2-L\delta)\delta\gamma} \log\left(\frac{1}{\eta}\right)$, where L, γ is the parameter associated with the loss function. The step must satisfy $\delta < \frac{2}{L}$. Therefore, the training energy consumption of user n in each global round is

$$E_n^{comp} = \kappa I_l C_n D_n f_n^2, \ \forall n \in \mathcal{N}_m \tag{6}$$

where κ is the effective switched capacitance.

2.2.2. Communication Model

After the user n completes the local training, the trained model is uploaded to the UAV by FDMA. According to Shannon's formula, the transmission rate of user n is

$$R_n = b_n \log_2\left(1 + \frac{g_n p_n}{N_0 b_n}\right), \ \forall n \in \mathcal{N}_m \tag{7}$$

where b_n is the bandwidth allocated to user n and p_n is the transmission power of user n.

We set the neural network model $\mathbf{w}$ size as s, so the communication energy consumption and delay of user n in each global round are

$$E_n^{comm} = p_n t_n = p_n \frac{s}{R_n}, \ \forall n \in \mathcal{N}_m \tag{8}$$

$$t_n = \frac{s}{R_n}, \ \forall n \in \mathcal{N}_m \tag{9}$$

According to [10], when the required global accuracy reaches ε_0, the global round needs to satisfy the condition: $I_g \geq \frac{2L^2}{\gamma^2 \xi} \log \frac{1}{\varepsilon_0} \frac{1}{1-\eta}$, so $I_g = \frac{2L^2}{\gamma^2 \xi} \log \frac{1}{\varepsilon_0} \frac{1}{1-\eta}$. So, the total energy consumption of users in the entire FL process is

$$E^{total} = I_g \sum_{n \in \mathcal{N}_m}^{|\mathcal{N}_m|} \left(E_n^{comm} + E_n^{comp}\right) \tag{10}$$

The total latency of user n is

$$T_n = I_g \left(\frac{I_l C_n D_n}{f_n} + t_n\right), \forall n \in \mathcal{N}_m \tag{11}$$

We set T as denoting the completion time of FL, for the sake of ensuring the FL learning performance, and we defined that users who participate in FL must meet the requirements: $T_n \leq T, \forall n \in \mathcal{N}_m$.

2.3. Problem Formulation

The battery capacity of the users is limited, and the energy consumption of users directly affects the users' experience. Therefore, this paper defines the total energy consumption of users as a part of the cost function. Because the performance of FL is related to the number of users participating, the more users participating, the faster the speed of FL convergence; meanwhile, the more data diversity of users participating in FL, the stronger the generalization ability of the model. Therefore, the reciprocal of the number of users participating in FL is defined as another part of the cost function, representing the performance of federated learning. So as to achieve a balance between the total energy consumption of users and the FL performance, the total cost function is defined as

$$C = E_{total} + \rho \frac{1}{N_m} \tag{12}$$

where N_m is number of users participating in FL and ρ is a weight coefficient.

Therefore, to achieve the balance between the total energy consumption and FL performance, the objective of this paper is to minimize the total cost function by jointly optimizing the UAV m position (horizontal placement $\mathbf{q}_m = \{x, y\}$, altitude h), user computation frequency $\mathbf{f} = [f_1, \cdots f_{N_m}]$, transmission power $\mathbf{p} = [p_1, \cdots p_{N_m}]$, transmission bandwidth

$\mathbf{b} = [b_1, \cdots b_{N_m}]$, transmission time $\mathbf{t} = [t_1 \cdots t_{N_m}]$ and local accuracy η within a given total FL completion time budget. The optimization problem can be expressed as

$$\begin{aligned}
\text{P1}: \quad & \min_{\mathbf{q}_m,\, h,\, \mathbf{f},\, \mathbf{t},\, \mathbf{p},\, \mathbf{b},\, \eta} \frac{a}{(1-\eta)} \left(\sum_{i \in \mathcal{N}_m}^{|\mathcal{N}_m|} \log\left(\frac{1}{\eta}\right) v C_i D_i f_i^2 + t_i p_i \right) + \frac{\rho}{N_m} \\
& \text{s.t. } \text{C1}: 0 \le f_i \le f_i^{\max}, \forall i \in \mathcal{N}_m \\
& \quad \text{C2}: 0 \le p_i \le p_i^{\max}, \forall i \in \mathcal{N}_m \\
& \quad \text{C3}: I_g\left(t_i + I_l \frac{C_i D_i}{f_i}\right) \le T, \forall i \in \mathcal{N}_m \\
& \quad \text{C4}: t_i \ge \frac{s}{b_i \log_2\left(1 + \frac{p_i g_i}{b_i N_0}\right)}, \forall i \in \mathcal{N}_m \\
& \quad \text{C5}: \|\mathbf{q}_m - \mathbf{q}_i\|_2^2 \le r^2, \forall i \in \mathcal{N}_m, \\
& \quad \text{C6}: h^{\min} \le h \le h^{\max} \\
& \quad \text{C7}: \sum_{i \in \mathcal{N}_m}^{|\mathcal{N}_m|} b_i \le B, b_i > 0, \forall i \in \mathcal{N}_m \\
& \quad \text{C8}: 0 \le \eta \le 1
\end{aligned} \tag{13}$$

where $a = \frac{2L^2}{\gamma^2 \zeta} \log \frac{1}{\varepsilon_0}$, $v = \frac{2}{(2 - L\delta)\delta\gamma}$ are constants. Constraints C1 and C2 indicate constraints on the computation frequency and transmission power. Constraint C3 indicates that the total latency of users participating in FL cannot exceed the preset maximum. Constraint C4 is the constraint on transmission delay, that is, the transmission of the model must be completed within the specified transmission time. Constraint C5 represents the position constraint of the UAV. The distance between the user and the UAV should not exceed the coverage range of the UAV. Constraint C6 restricts the flying altitude range of the UAV. If the altitude is too low, there will be too few users to participate; however, if the altitude is too high, the competition for wireless resources will be fierce, leading to an increase in users' energy consumption, and both of them will slow down the convergence rate of FL. Constraint C7 represents that the total bandwidth allocated to all users within the UAV's coverage range cannot exceed the preset total bandwidth B. Constraint C8 specifies the constraint range of local accuracy.

3. Joint Optimization Algorithm

Because the above problem is not convex, it is difficult to solve it directly. Moreover, the UAV's altitude affects the users' access, but the number of users depends on the distribution of the users, so we first fixed the altitude of the UAV, then, the remaining variables $\mathbf{q}_m$, η, $\mathbf{f}$, $\mathbf{t}$, $\mathbf{p}$, $\mathbf{b}$ are assigned a value satisfying the feasible domain. Then, we transformed it into three subproblems: UAV horizontal placement, local accuracy and computation and communication resources, and used the corresponding algorithm to solve them. For the sake of understanding, the dependency relationships among algorithms are shown in Figure 2.

3.1. Subproblem 1: UAV Horizontal Placement

When h, $\mathbf{f}$, $\mathbf{t}$, $\mathbf{p}$, $\mathbf{b}$, η are determined, since the optimization of UAV horizontal placement only affects the transmission energy consumption of users, we formulated the P2 problem

$$\begin{aligned}
\text{P2}: \quad & \min_{\mathbf{q}_m} \sum_{i \in \mathcal{N}_m}^{|\mathcal{N}_m|} p_i \frac{s}{R_i} \\
& \text{s.t. } \text{C1}: t_i \ge \frac{s}{R_i}, \forall i \in \mathcal{N}_m \\
& \quad \text{C2}: \|\mathbf{q}_m - \mathbf{q}_i\|_2^2 \le r^2, \forall i \in \mathcal{N}_m
\end{aligned} \tag{14}$$

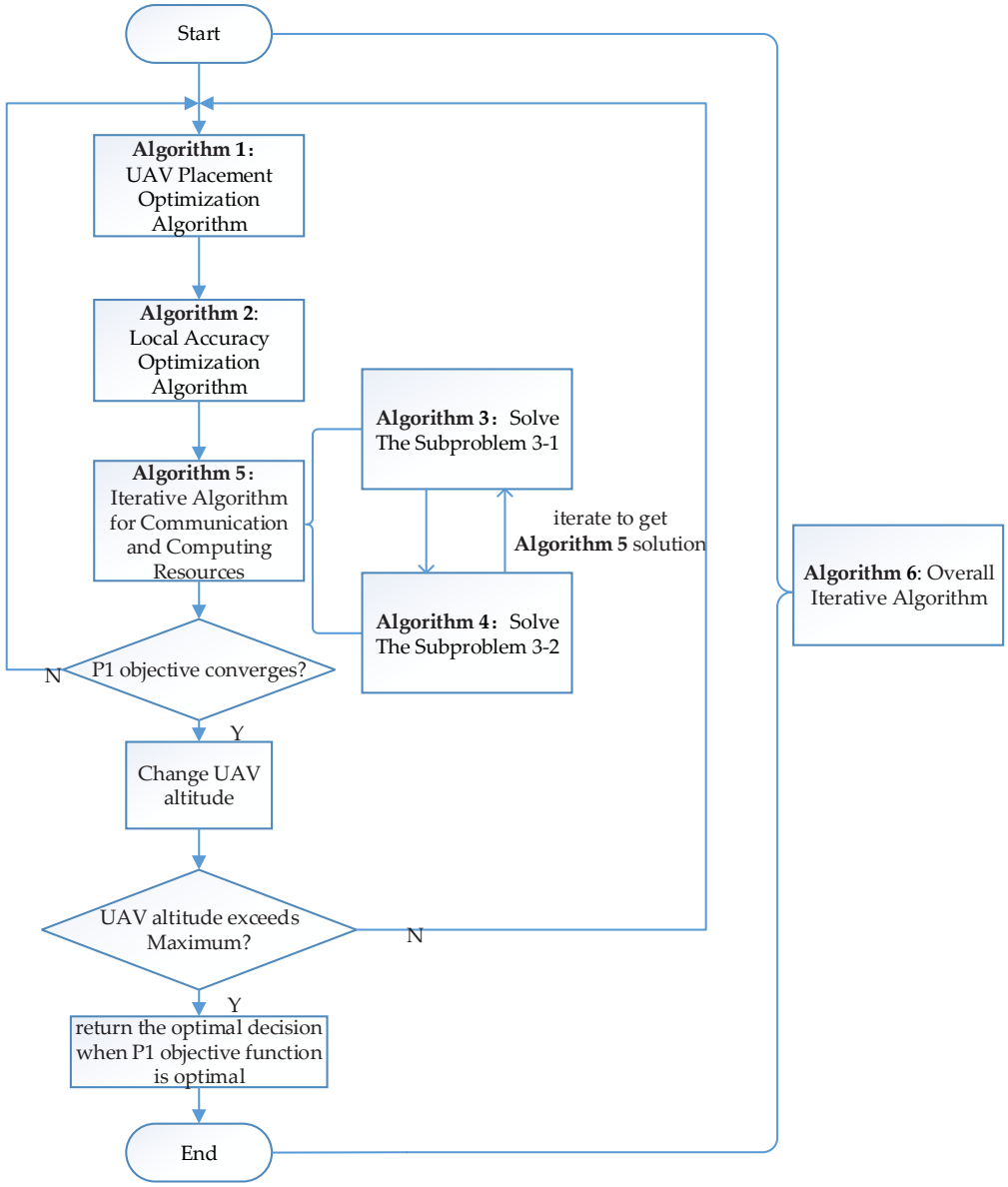


Figure 2. The interactions and dependency relationships among algorithms.

Because P2 is a non-convex problem, it is difficult to solve it directly, so we introduced slack variables β, and converted it to the P3 problem.

$$\begin{aligned} \text{P3}: \quad & \min_{\mathbf{q}_m, \boldsymbol{\beta}} \sum_{i \in \mathcal{N}_m}^{|\mathcal{N}_m|} p_i s \beta_i \\ & \text{s.t. C1}: s\beta_i \le t_i, \forall i \in \mathcal{N}_m \\ & \text{C2}: b_i \log_2\left(1 + \frac{p_i g_0}{b_i N_0 \left(\|\mathbf{q}_m - \mathbf{q}_i\|_2^2 + h^2\right)}\right) \ge \frac{1}{\beta_i}, \forall i \in \mathcal{N}_m \\ & \text{C3}: \|\mathbf{q}_m - \mathbf{q}_i\|_2^2 \le r^2, \forall i \in \mathcal{N}_m \end{aligned} \tag{15}$$

Since constraint C2 in P3 is not convex, so we introduced a variable $S_{m,i} = \|\mathbf{q}_m - \mathbf{q}_i\|_2^2$, and made the constraints C2 at the feasible solution $S_{m,i}^0 = \|\mathbf{q}_m^0 - \mathbf{q}_i\|_2^2$ use a first-order Taylor expansion.

$$b_i \log_2\left(1+\frac{p_i g_0}{b_i N_0\left(S_{m,i}+h^2\right)}\right) \geq \boldsymbol{\lambda}\left(S_{m,i}-S_{m,i}^0\right)+\boldsymbol{\kappa} \tag{16}$$

$$\boldsymbol{\lambda} = -\frac{b_i g_0 p_i \log_2(e)}{N_0 b_i\left(S_{m,i}^0+h^2\right)\left(S_{m,i}^0+h^2+\frac{g_0 p_i}{N_0 b_i}\right)} \tag{17}$$

$$\boldsymbol{\kappa} = b_i \log_2\left(1+\frac{g_0 p_i}{N_0 b_i\left(S_{m,i}^0+h^2\right)}\right) \tag{18}$$

where $\boldsymbol{\lambda}$, $\boldsymbol{\kappa}$ are intermediate variables. Equation (16) is substituted into (15), and then the P3 optimization problem is transformed into the P4 problem

$$\begin{aligned} \text{P4}: \quad & \min_{\mathbf{q}_m, \boldsymbol{\beta}} \sum_{i\in\mathcal{N}_m}^{|\mathcal{N}_m|} p_i s\beta_i \\ & \text{s.t. C1}: s\beta_i \leq t_i, \forall i \in \mathcal{N}_m \\ & \quad \text{C2}: \boldsymbol{\lambda}\left(S_{m,i}-S_{m,i}^0\right)+\boldsymbol{\kappa} \geq \tfrac{1}{\beta_i}, \forall i \in \mathcal{N}_m \\ & \quad \text{C3}: \|\mathbf{q}_m-\mathbf{q}_i\|_2^2 \leq r^2, \forall i \in \mathcal{N}_m \end{aligned} \tag{19}$$

In this case, the P4 problem becomes a convex problem and can be settled by the successive convex approximation (SCA) technique. When the UAV arrives at the new placement, the UAV coverage placement will be changed. Due to the C2 constraint, the original users are still within the scope of the UAV, but new users may join. At this time, the values of each variable are reinitialized and the algorithm is reiterated. The details are shown in Algorithm 1.

Algorithm 1: UAV Placement Optimization Algorithm

Input: Initial feasible UAV placement $\mathbf{q}_m^0 = (x^0, y^0)$, iteration $r_1 = 0$, maximum iterations $r_1^{\max}$, step size σ

Output: Optimal UAV location $\mathbf{q}_m^*$

```
while r_1 ≤ r_1^max do
    Use CVX to compute P4 optimal UAV location q_m^{r_1'}
    Set q_m^{r_1+1} = q_m^{r_1} + σ(q_m^{r_1'} − q_m^{r_1})
    if the access users has changed
        Reinitialize f, t, p, b
        continue
    end if
    if q_m^{r_1+1} is a convergent solution of P3
        break
    else if
        Set r_1 = r_1 + 1
    end if
end while
```

3.2. Subproblem 2: Local Accuracy

When h, $\mathbf{q}_m$, $\mathbf{f}$, $\mathbf{t}$, $\mathbf{p}$, $\mathbf{b}$ are determined, the η optimization problem can be expressed as the P5 problem

$$\begin{aligned} \text{P5}: \quad & \min_{\eta} \frac{\lambda_1 \log_2\left(\frac{1}{\eta}\right)+\lambda_2}{(1-\eta)} \\ & \text{s.t. C1}: I_g\left(t_i + I_l \tfrac{C_i D_i}{f_i}\right) \leq T, \forall i \in \mathcal{N}_m \\ & \quad \text{C2}: 0 \leq \eta \leq 1 \end{aligned} \tag{20}$$

where $\lambda_1 = a\sum_{i\in\mathcal{N}_m}^{|\mathcal{N}_m|}\kappa C_i D_i f_i^2$, $\lambda_2 = a\sum_{i\in\mathcal{N}_m}^{|\mathcal{N}_m|} t_i p_i$ are constants. The constraint C1 is equivalent to $t_i \le v(\eta_i)$, where $v(\eta) = \frac{1-\eta}{a}T + \frac{C_i D_i \log(\eta)v}{f_i}$, because $v(\eta)'' \le 0$, so $v(\eta)$ is a convex function, and the authors of [10] provided specific proof. Therefore, constraint C1 can be converted to $\eta^{\min} \le \eta \le \eta^{\max}$, where $\eta^{\max} = \min_{i\in\mathcal{N}_m}\eta_i^{\max}$, $\eta^{\min} = \max_{i\in\mathcal{N}_m}\eta_i^{\min}$. So, the P5 problem is transformed into the P6 form.

$$\begin{aligned} \text{P6}: \quad & \min_{\eta} \frac{\lambda_1 \log\left(\frac{1}{\eta}\right)+\lambda_2}{(1-\eta)} \\ & \text{s.t. C1}: \eta^{\min} \le \eta \le \eta^{\max} \end{aligned} \tag{21}$$

Obviously, the P6 problem is a fraction form at this time, so it is difficult to solve it directly. Based on the work of [10,28], the P6 problem is equivalent to finding the root of the nonlinear function $H(\zeta)$.

$$H(\zeta) = \min_{\eta^{\min}\le\eta\le\eta^{\max}} \lambda_1 \log(1/\eta) + \lambda_2 - \zeta(1-\eta) \tag{22}$$

We can therefore use the Dinkelbach Method to solve the above question. The details are shown in Algorithm 2.

Algorithm 2: Local Accuracy Optimization Algorithm

Input: Initial $\zeta = \zeta^{(0)} > 0$, $\eta^{\min}$, $\eta^{\max}$, iteration number $r_2 = 0$, and set the accuracy e
Output: η^*

repeat
  Computing the optimal $\eta^* = \lambda_1/\zeta^{(n)}$
  if $\eta^* < \eta^{\min}$
    $\eta^* = \eta^{\min}$
  else if $\eta^* > \eta^{\max}$
    $\eta^* = \eta^{\max}$
  end if
  Update $\zeta^{(n+1)} = (\lambda_1 \log_2(1/\eta^*) + \lambda_2)/(1-\eta^*)$
  Set $r_2 = r_2 + 1$
until $\left|H\left(\zeta^{(n+1)}\right)\right| / \left|H\left(\zeta^{(n)}\right)\right| < e$

3.3. Subproblem 3: User Computation and Communication Resources

When $\mathbf{q}_m$, h, η are determined, Subproblem 3 can be expressed as the P7 problem.

$$\begin{aligned} \text{P7}: \quad & \min_{\mathbf{f},\mathbf{t},\mathbf{p},\mathbf{b}} \frac{a}{(1-\eta)} \sum_{i\in\mathcal{N}_m}^{|\mathcal{N}_m|} \left(v\log\left(\frac{1}{\eta}\right) C_i D_i f_i^2 + p_i t_i\right) \\ & \text{s.t. C1}: 0 \le f_i \le f_i^{\max}, \forall i \in \mathcal{N}_m \\ & \quad \text{C2}: 0 \le p_i \le p_i^{\max}, \forall i \in \mathcal{N}_m \\ & \quad \text{C3}: I_g\left(t_i + I_l \frac{C_i D_i}{f_i}\right) \le T, \forall i \in \mathcal{N}_m \\ & \quad \text{C4}: t_i b_i \log_2\left(1 + \frac{p_i g_i}{b_i N_0}\right) \ge s, \forall i \in \mathcal{N}_m \\ & \quad \text{C5}: \sum_{i\in\mathcal{N}_m}^{|\mathcal{N}_m|} b_i \le B, b_i \ge 0, \forall i \in \mathcal{N}_m \end{aligned} \tag{23}$$

Since P7 is a non-convex problem, it is difficult to solve it directly. So this paper further divides subproblem 3 into two optimization subproblems: subproblem 3-1 and subproblem 3-2.

3.3.1. Subproblem 3-1: **f**, **t**, **p** Optimization Problem

When **b** is determined, the **f**, **t**, **p** optimization problem can be expressed as

$$\begin{aligned} \text{P7-1}: \quad & \min_{\mathbf{f},\,\mathbf{t},\,\mathbf{p}} \frac{a}{(1-\eta)} \sum_{i\in\mathcal{N}_m}^{|\mathcal{N}_m|} \left(v \log\left(\frac{1}{\eta}\right) C_i D_i f_i^2 + p_i t_i \right) \\ & \text{s.t. } \text{C1}: 0 \le f_i \le f_i^{\max}, \forall i \in \mathcal{N}_m \\ & \quad \text{C2}: 0 \le p_i \le p_i^{\max}, \forall i \in \mathcal{N}_m \\ & \quad \text{C3}: I_g \left(t_i + I_l \frac{C_i D_i}{f_i} \right) \le T, \forall i \in \mathcal{N}_m \\ & \quad \text{C4}: t_i b_i \log_2\left(1 + \frac{p_i g_i}{b_i N_0}\right) \ge s, \forall i \in \mathcal{N}_m \end{aligned} \tag{24}$$

According to constraint C3, we obtain $f_i \ge \frac{I_l C_i D_i}{\frac{T}{I_g} - t_i}$, since the higher the frequency f, the greater the training energy consumption, so we set $f_i = \frac{I_l C_i D_i}{\frac{T}{I_g} - t_i}$. According to constraint C4, we obtain $p_i \ge \frac{N_0 b_i}{g_i}\left(2^{\frac{s}{t_i b_i}} - 1\right)$, so we set $p_i = \frac{N_0 b_i}{g_i}\left(2^{\frac{s}{t_i b_i}} - 1\right)$. We substitute $f_i = \frac{I_l C_i D_i}{\frac{T}{I_g} - t_i}$ and $p_i = \frac{N_0 b_i}{g_i}\left(2^{\frac{s}{t_i b_i}} - 1\right)$ into (23), and the P7-1 problem is transformed into:

$$\begin{aligned} \text{P8}: \quad & \min_{\mathbf{f},\,\mathbf{t},\,\mathbf{p}} \frac{a}{(1-\eta)} \sum_{i\in\mathcal{N}_m}^{|\mathcal{N}_m|} \left(v \log\left(\frac{1}{\eta}\right) C_i D_i \left(\frac{I_l C_i D_i}{\frac{T}{I_g} - t_i^*} \right)^2 + \frac{N_0 b_i}{g_i} \left(2^{\frac{s}{t_i^* b_i}} - 1 \right) t_i^* \right) \\ & \text{s.t. } \text{C1}: 0 \le \frac{I_l C_i D_i}{\frac{T}{I_g} - t_i} \le f_i^{\max}, \forall i \in \mathcal{N}_m \\ & \quad \text{C2}: 0 \le \frac{N_0 b_i}{g_i}\left(2^{\frac{s}{t_i b_i}} - 1\right) \le p_i^{\max}, \forall i \in \mathcal{N}_m \end{aligned} \tag{25}$$

According to constraints C1 and C2, we can obtain the maximum and minimum values of t_i, so the P8 problem is further converted the P9 problem:

$$\begin{aligned} \text{P9}: \quad & \min_{\mathbf{t}} \frac{a}{(1-\eta)} \sum_{i\in\mathcal{N}_m}^{|\mathcal{N}_m|} \left(v \log\left(\frac{1}{\eta}\right) C_i D_i \left(\frac{I_l C_i D_i}{\frac{T}{I_g} - t_i} \right)^2 + \frac{N_0 b_i}{g_i} \left(2^{\frac{s}{t_i b_i}} - 1 \right) t_i \right) \\ & \text{s.t. } \text{C1}: t_i^{\min} \le t_i \le t_i^{\max}, \forall i \in \mathcal{N}_m \end{aligned} \tag{26}$$

For the P9 problem, when t_i satisfies $\left|\partial E_n^{comp}/\partial t_n\right| = |\partial E_n^{comm}/\partial t_n|$, we can obtain the optimal solution t_i, and further obtain f_i^* and p_i^*.

Proof: The training energy consumption and communication energy consumption of user n in each global round separately are:

$$E_n^{comp} = \kappa I_l C_n D_n f_n^2 = \kappa I_l C_n D_n \left(\frac{I_l C_n D_n}{\frac{T}{I_g} - t_n} \right)^2 \tag{27}$$

$$E_n^{comm} = p_n t_n = \frac{N_0 b_n}{g_n}\left(2^{\frac{s}{t_n b_n}} - 1\right) t_n \tag{28}$$

Equation (27) differentiates the transmission time t_n to obtain:

$$\frac{\partial E_n^{comp}}{\partial t_n} = 2 {I_l}^3 \kappa {C_n}^3 {D_n}^3 \left(\frac{T}{I_g} - t_n \right)^{-3} \ge 0 \tag{29}$$

so the training energy consumption E_n^{comp} is an increasing function of t_n.

Equation (28) differentiates the transmission time t_n to obtain:

$$\frac{\partial E_n^{comm}}{\partial t_n} = \frac{N_0 b_n}{g_n}\left(2^{\frac{s}{t_n b_n}} - 1\right) - \frac{N_0}{g_n} 2^{\frac{s}{t_n b_n}} \ln(2) \left(\frac{s}{t_n} \right) \tag{30}$$

however, we cannot find the relation between (30) and zero, so we can find the second derivative:

$$\frac{(\partial E_n^{comm})^2}{\partial {t_n}^2} = \frac{N_0}{g_n} 2^{\frac{s}{t_n b_n}} (\ln(2))^2 \frac{s^2}{b_n {t_n}^3} \geq 0 \tag{31}$$

So $\partial E_n^{comm}/\partial t_n$ is an increasing function of t_n, and when t_n tends to infinity, $\partial E_n^{comm}/\partial t_n = 0$, for all t_n, $\partial E_n^{comm}/\partial t_n \leq 0$, so the training energy consumption E_n^{comm} is a decreasing function of t_n. Take the absolute value of $\partial E_n^{comp}/\partial t_n$ and $\partial E_n^{comm}/\partial t_n$, when one of them is bigger, such as $\left|\partial E_n^{comp}/\partial t_n\right| > |\partial E_n^{comm}/\partial t_n|$, we can reduce the value of t_n, in this case the training energy consumption becomes smaller and the communication energy consumption becomes larger. However, since $\left|\partial E_n^{comp}/\partial t_n\right| > |\partial E_n^{comm}/\partial t_n|$, the reduction in the training energy consumption is more than the increase in the communication energy consumption. In general, the energy consumption of user n is reduced. Since E_n^{comp} and E_n^{comm} have nice monotone properties about t_n, so we can apply the bisection method to find t_n^*. The details are shown in Algorithm 3. □

Algorithm 3: Solve The Subproblem 3-1: **f**, **t**, **p**

Input: $\mathbf{t}^{\min}$, $\mathbf{t}^{\max}$, user set $\mathcal{N}_m$, iteration $r_3 = 0$, maximum iterations $r_3^{\max}$, and set the accuracy e_1
Output: $\mathbf{f}^*$, $\mathbf{t}^*$, $\mathbf{p}^*$

for $n = 0, \ldots, N_m$ **do**
  while $r_3 \leq r_3^{\max}$ **do**
    Set $t_n = \left(t_n^{\max} + t_n^{\min}\right)/2$
    if $\left|\left|\partial E_n^{comp}/\partial t_n\right| - |\partial E_n^{comm}/\partial t_n|\right| \leq e_1$ or $r_3 > r_3^{\max}$
      $t_n^* = t_n$
      return t_n^*
    else if $\left|\partial E_n^{comp}/\partial t_n\right| > |\partial E_n^{comm}/\partial t_n|$
      $t_n^{\max} = t_n$
      Set $r_3 = r_3 + 1$
    else if $\left|\partial E_n^{comp}/\partial t_n\right| < |\partial E_n^{comm}/\partial t_n|$
      $t_n^{\min} = t_n$
      Set $r_3 = r_3 + 1$
    end if
  end while

3.3.2. Subproblem 3-1: **b** Optimization Problem

When **f**, **t**, **p** are determined, the **b** optimization problem can be expressed as

$$\begin{aligned} \text{P7-2}: \quad & \min_{\mathbf{b}} \sum_{i \in \mathcal{N}_m}^{|\mathcal{N}_m|} \frac{b_i t_i N_0}{g_i} \left(2^{\frac{s}{t_i b_i}} - 1\right) \\ & \text{s.t. C1}: b_i \geq 0, \forall i \in \mathcal{N}_m \\ & \text{C2}: \sum_{i \in \mathcal{N}_m}^{\mathcal{N}_m} b_i = B, \forall i \in \mathcal{N}_m \end{aligned} \tag{32}$$

We can use the Karush–Kuhn–Tucker conditions (KKT) to solve (32), the optimal bandwidth can be expressed as

$$b_i^* = \frac{s \ln 2}{t_i \left[1 + \mathcal{W}\left(\frac{g_i \mu^* - B t_i N_0}{B t_i N_0 e}\right)\right]} \tag{33}$$

where $\mathcal{W}(\bullet)$ is the Lambert *W*-function. The Lagrange multiplier vector μ^* should satisfy the conditions:

$$k(\mu^*) = \sum_{i \in \mathcal{N}_m}^{|\mathcal{N}_m|} \frac{s \ln 2}{t_i \left[1 + \mathcal{W}\left(\frac{g_i \mu^* - B t_i N_0}{B t_i N_0 e}\right)\right]} = B \tag{34}$$

Proof: Since the P7-2 is a convex problem, it can be solved by using the KKT conditions. The Lagrange function is

$$L(\mathbf{b}, \mu) = \sum_{i \in \mathcal{N}_m}^{|\mathcal{N}_m|} \frac{b_i t_i N_0}{g_i} \left(2^{\frac{s}{t_i b_i}} - 1\right) + \mu \left(\sum_{i \in \mathcal{N}_m}^{|\mathcal{N}_m|} b_i - B\right) \tag{35}$$

where μ^* is the Lagrange multiplier associated with constraint C2. The first order derivative of (35) with respect b_i to is

$$\frac{\partial L(\mathbf{b}, \mu)}{\partial b_i} = \frac{N_0}{g_i t_i} \left(e^{\frac{(\ln 2)s}{t_i b_i}} - 1 - \frac{\ln(2) s}{t_i b_i} e^{\frac{(\ln 2)s}{t_i b_i}}\right) + \mu \tag{36}$$

we can obtain b_i^* as the unique solution to $\partial L(\mathbf{b}, \mu)/\partial b_i = 0$. □

Since the Lambert *W*-function is an increase function, as a result, $k(\mu^*)$ is a decrease function of μ^*. So, we can use the bisection method to find μ^*, and then obtain $\mathbf{b}^*$. The details are shown in Algorithm 4.

Algorithm 4: Solve The Subproblem 3-2: **b**

Input: $\mu^{\min} = 0$, $\mu^{\max}$, $\mathbf{t}^*$
Output: μ^*, $\mathbf{b}^*$
repeat
  Set $\mu = (\mu^{\min} + \mu^{\max})/2$
  if $k(\mu^*) = B$
    $\mu^* = \mu$
    return μ^*
  else if $k(\mu^*) > B$
    $\mu^{\min} = \mu$
  else if $k(\mu^*) < B$
    $\mu^{\max} = \mu$
  end if
end while

Because the optimization of subproblem 3-2 will cause the change in bandwidth **b**, which will affect **f**, **t**, **p** in subproblem 3-1, it is necessary to iterate between subproblem 3-1 and subproblem 3-2. The details are shown in Algorithm 5.

Algorithm 5: Iterative Algorithm for Communication and Computing Resources

Input: $\mathbf{f}^{(0)}\mathbf{t}^{(0)}\mathbf{p}^{(0)}\mathbf{b}^{(0)}$ iteration $r_4 = 0$, maximum iterations $r_4^{\max}$
Output: $\mathbf{f}^*\mathbf{t}^*\mathbf{p}^*\mathbf{b}^*$
while $r_4 < r_4^{\max}$
  Fixed **b**, according to Algorithm 3 to obtain **f**, **t**, **p**
  Fixed **f**, **t**, **p**, according to Algorithm 4 to obtain **b**
  Set $r_4 = r_4 + 1$
end while

Through Algorithms 1,2 and 5 iterations, the final converged solution is obtained, and then according to the $\Delta h_{\min}$ change the altitude of the UAV, repeat three subproblem iterative process, until the UAV altitude h exceeds $h^{\max}$. Eventually, return $\mathbf{q}_m^*$, h^*, $\mathbf{f}^*$, $\mathbf{t}^*$, $\mathbf{p}^*$, $\mathbf{b}^*$, η^* when the P1 objective function is optimal. The overall iterative algorithm flow is shown in Algorithm 6.

Algorithm 6: Overall Iterative Algorithm

1: Initial feasible solution $\mathbf{q}_m^{(0)}$, $\mathbf{f}^{(0)}$, $\mathbf{t}^{(0)}$, $\mathbf{p}^{(0)}$, $\mathbf{b}^{(0)}$, $\eta^{(0)}$
2: **repeat**
3: Set $h = h^{\min}$
4: **repeat**
5: Fixed $\mathbf{f}^{(j)}$, $\mathbf{t}^{(j)}$, $\mathbf{p}^{(j)}$, $\mathbf{b}^{(j)}$, $\eta^{(j)}$, according to Algorithm 1 to obtain $\mathbf{q}_m^{(j+1)}$
6: Fixed $\mathbf{f}^{(j)}$, $\mathbf{t}^{(j)}$, $\mathbf{p}^{(j)}$, $\mathbf{b}^{(j)}$, $\mathbf{q}_m^{(j+1)}$, according to Algorithm 2 to obtain $\eta^{(j+1)}$
7: Fixed $\mathbf{q}_m^{(j+1)}$, $\eta^{(j+1)}$, according to Algorithm 5 to obtain $\mathbf{f}^{(j+1)}$, $\mathbf{t}^{(j+1)}$, $\mathbf{p}^{(j+1)}\mathbf{b}^{(j+1)}$
8: Set $j = j + 1$
9: **until** P1 objective converges
10: Set $h = h + \Delta h_{\min}$
11: **until** $h > h^{\max}$
12: **return** $\mathbf{q}_m^*$, h^*, $\mathbf{f}^*$, $\mathbf{t}^*$, $\mathbf{p}^*$, $\mathbf{b}^*$, η^* when P1 objective function is optimal

4. Simulation Results and Performance Analysis

In this paper, we used python to simulate the proposed algorithm, and used pytorch to build the convolutional neural network to verify the performance of FL. In our simulations, we deploy $N = 20$ users uniformly in a square area of size 250 m $\times$ 250 m. In addition, the data distribution among users is non-IID, we used the MNIST dataset that consists of handwritten numbers "0" through "9" to train the neural network, and a total of 60,000 labeled training data samples. For data distribution processing between users, we first sorted all data samples by their digit labels, divided them into 200 shards of size 300, and then assigned each user with eight shards. So, each user obtains the data samples with no more than eight types of digits, with a total size of 2400. Other simulation parameters are shown in Table 2.

Table 2. Simulation Parameters.

Parameter	Value
Maximum Bandwidth of UAV B	1 MHz
Maximum Transmission Power $p^{\max}$	10 mW
Maximum Calculated Frequency $f^{\max}$	2 GHz
CPU of User C_n	$[1, 3] \times 10^4$ cycle/sample
Noise Power Spectral Density N_0	-174 dBm/Hz
User Dataset Size D_n	2400
Effective Switched Capacitance κ	10^{-28}
Loss Function Parameters	$\gamma = 2$, $L = 2$, $\delta = 1/4$, $\xi = 1/3$

Next, we compared the algorithm proposed in this paper with three algorithms, including: (1) the algorithm in [23] (UAV altitude fixed). In [23], the UAV altitude is the highest, that is, all users in the UAV-covered area; (2) The baseline algorithm that does not optimize local accuracy η is called the FLA in this paper, where the local accuracy is fixed; (3) The baseline algorithm that does not optimize the transmission time is called FTT in this paper, where the transmission time is fixed.

Figure 3a,b show the system cost and the overall energy consumption of users when the required FL completion time T increases from 100 to 200, respectively, where the model size s is 50 kbit and the global accuracy ε_0 is 0.001. As the required FL completion time T increases, so the four algorithms show a downward trend as users have more time to train

and upload, which reduces the resource competition among users. When T is small, the UAV in [23] is a fixed height, and as the UAV altitude is not optimized, so the total system cost and the total energy consumption of users are very high. Because the algorithm FLA does not optimize the local accuracy and the algorithm FTT does not optimize the transmission time, the system total cost and the total energy consumption of users are higher than our proposed algorithm. In Figure 3b, with the required FL completion time T increases, the total energy consumption of users decreases, and the learning performance plays a dominant role at this time. Therefore, the altitude of the UAV is increased, and the coverage area is expanded to reduce the cost of learning, thus the number of users participating in learning is increased. Therefore, as the required FL completion time increases, the number of participating users increases and the total energy consumption of users decreases. When the number of participants increases to a certain level, the diversity of the user dataset participating in learning is sufficient. If the number of users is increased on this basis, the effect of learning improvement is not obvious, but will occupy wireless resources and the use energy consumption will rise sharply. From the above analysis, our proposed algorithm has the fewest users participating in learning when T is 100, it only needs to compare the learning performance of our proposed algorithm and that in [23].

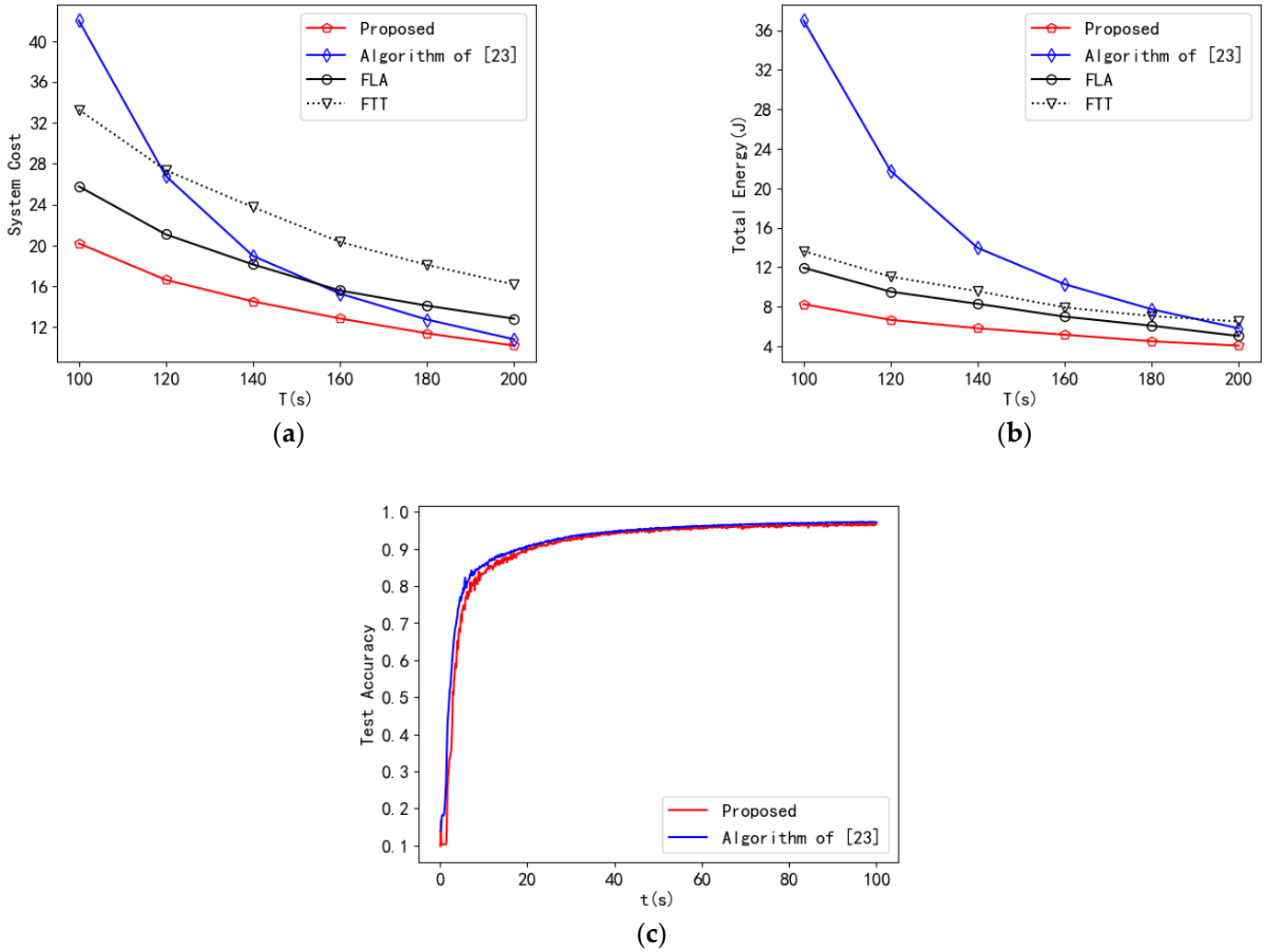


Figure 3. Total Completion Time Influence on Performance: (**a**) total system cost; (**b**) total energy consumption of users; (**c**) learning performance.

When T is 100, we can obtain the global rounds and local update rounds of the two algorithms according to the optimal local accuracy and preset global accuracy. The time of each global round can be approximately obtained on the basis of T. Since it only verifies the diversity of the data contained in both, the typical FedAvg algorithm in FL is used for training. As shown in Figure 3c, since the algorithm in [23] covers all users, so the convergence speed is faster than our proposed algorithm, but from the final convergence results, the final convergence accuracy of the two algorithms is only slightly different. However, our proposed algorithm can greatly reduce the total energy consumption of users under the condition of a lower required FL completion time. Therefore, the user data covered by our proposed algorithm basically contain all the data features of the overall dataset, if the user number is increased, the final learning performance will be little affected, but the total energy consumption of users will be increased. Through the above analysis, our proposed algorithm can not only guarantee the training performance but also reduce the total energy consumption of users under the condition of total completion time variation.

Figure 4 a,b show the system cost and the overall energy consumption of users when the global model accuracy ε_0 increases from 0.001 to 0.1, respectively, where the model size s is 50 kbit and total completion time T is 120. From Figure 4a,b, when the required global model accuracy decreases, the global rounds of users become less. Indirectly, the four algorithms' total cost function and the total energy consumption of users are decreased. When the global model accuracy changes to 0.05, the gap between the algorithm in [23] and our proposed algorithm is very small. This is because when the required global model accuracy is very small, users only need to train several rounds to reach the required accuracy, which reduces the users' total energy consumption. As a result, the UAV altitude optimized by our proposed algorithm is close to that of the algorithm in [23]. The total system cost and total energy consumption of algorithm FLA and FTT are also higher than our proposed algorithm. Based on previous analysis, because our proposed algorithm will have more users as the global model accuracy increases, so it only needs to compare the learning performance of our proposed algorithm and in [23], when the global model accuracy is 0.001. As shown in Figure 4c, our proposed algorithm covers enough diversity of user data, so the final test accuracy of the two is only slightly different. However, our proposed algorithm reduces the total energy consumption of users when the global accuracy is highly required. In addition, Figure 4c compared with Figure 3c, since T in Figure 4c is 120, our proposed algorithm covers more users than that in Figure 3c. Therefore, in the early stage of training, the convergence gap between our proposed algorithm and that in [23] is smaller than that in Figure 3c. Moreover, the convergence rate of our proposed algorithm is very close to the algorithm in [23]. This also verifies the conclusion that the more users, the faster the convergence speed, but this has little influence on the final convergence accuracy within the time expectation. In conclusion, our proposed algorithm can guarantee the training performance while reducing the total energy consumption of users under the condition of the global accuracy changes.

Figure 5a,b show the system cost and the total energy consumption of users when the model size s increases from 30 kbit to 80 kbit, respectively, where the global model accuracy ε_0 is 0.001 and total completion time T is 120. From the Figure 5a,b, as the model size increases, the users need more resources to transmit data, so the four algorithms' system cost and the total energy consumption of users are increased. Because the UAV altitude is not optimized in [23], as the model size increases, wireless resources' competition among users becomes more intense, resulting in a sharp rise in system cost and the total energy consumption of users. However, our proposed algorithm will appropriately reduce the UAV altitude to reduce resource competition among users. Therefore, the total system cost and total energy consumption of [23] are higher than our proposed algorithm. Due to the influence of local accuracy and transmission time, the system cost and total energy consumption of algorithm FLA and FTT are also higher than our proposed algorithm. When the model size is 80 kbit, our proposed algorithm has the least number of participating users, so it only needs to compare the learning performance at 80 kbit. As shown in

Figure 5c, because there are more participating users in [23], so the convergence speed is faster than that of our proposed algorithm. However, within the total completion time 120, there is little difference in the final convergence accuracy of the two algorithms. Therefore, our proposed algorithm not only guarantees the training performance but also reduces the total energy consumption of users when the model size changes, and can adjust the number of participants in learning according to the model size.

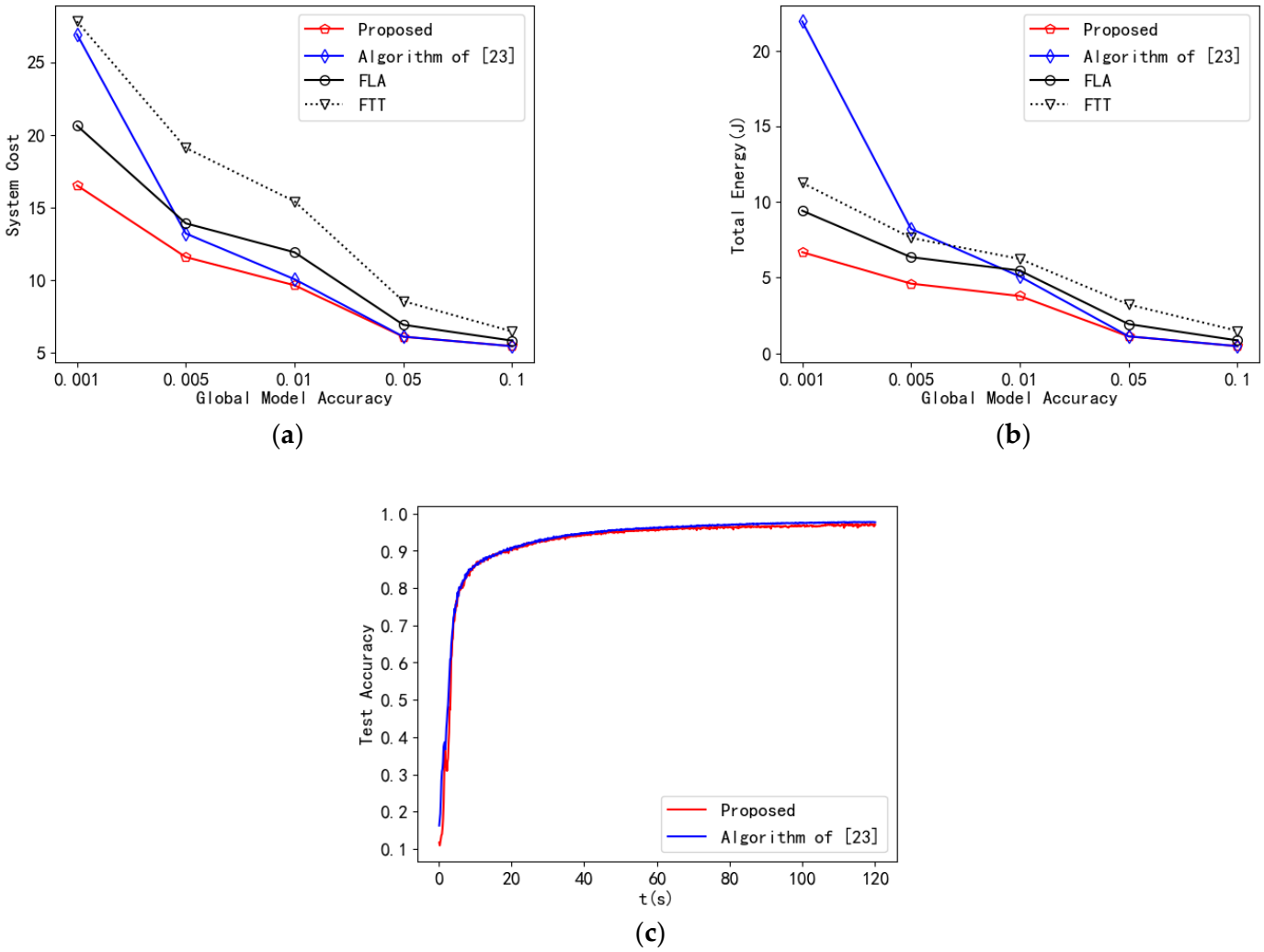


Figure 4. Global Model Accuracy Influence on Performance: (**a**) total system cost; (**b**) total energy consumption of users; (**c**) learning performance.

Figure 6 compares the effects of different total bandwidths on the system cost and user total energy consumption of our proposed algorithm. The total bandwidths are set at 1.5 MHz, 1 MHz and 0.5 MHz, respectively. From Figure 6, with the increase in total bandwidth, the total system cost and the total energy consumption of users are decreased. This is because when the total bandwidth increases, users can have more wireless resources, reducing the wireless resources' competition among users, the total energy consumption of users will be decreased, which further leads to more users joining the learning process and so the system cost will also be decreased.

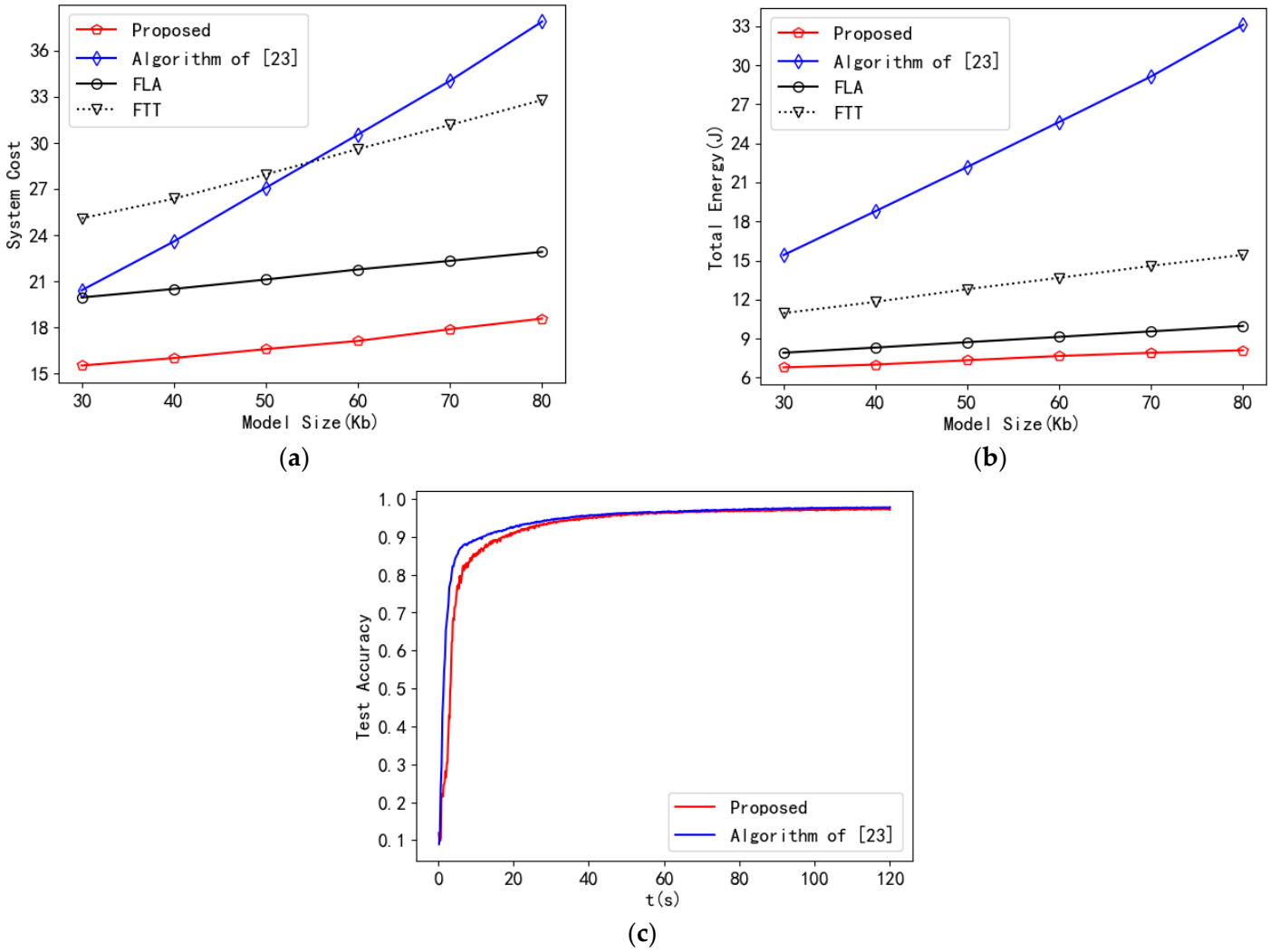


Figure 5. Model Size Influence on Performance: (**a**) total system cost; (**b**) total energy consumption of users; (**c**) learning performance.

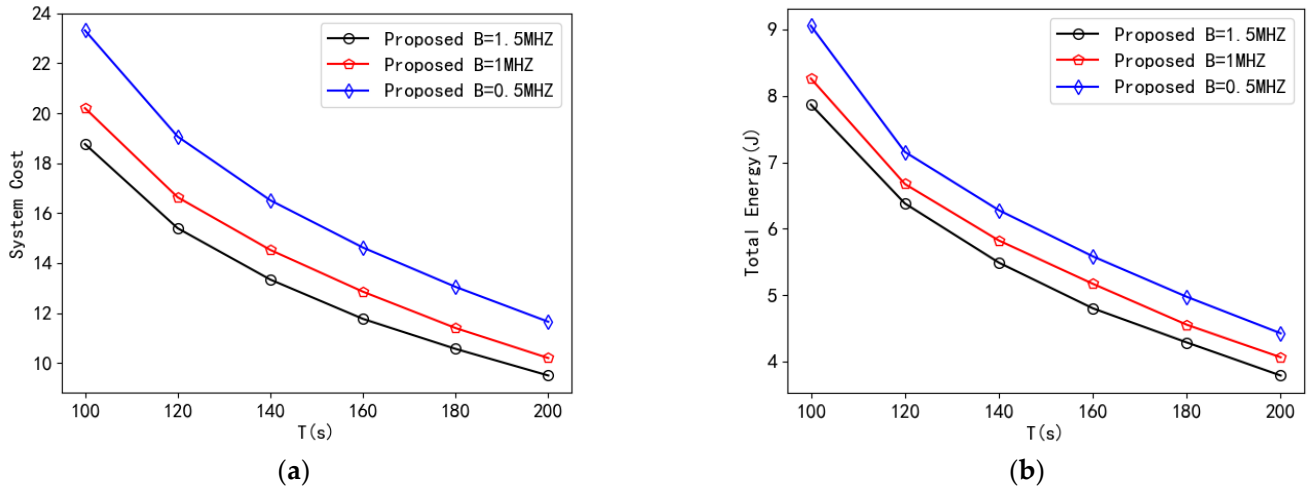


Figure 6. Total bandwidth Influence on Total System Cost and Total Energy Consumption: (**a**) total system cost; (**b**) total energy consumption of users.

5. Conclusions

In this paper, we investigate the FL application scenario of UAV communication network. By taking the total energy consumption and the reciprocal of the participating user numbers as the optimization objective, we propose a resource allocation scheme to jointly optimize the UAV position (horizontal placement, altitude), local accuracy and user computation and communication resource (computation frequency, communication power, communication bandwidth, communication time).

Because the formulated problem is difficult to solve directly, we cleverly decompose it into three sub-problems: UAV horizontal placement, local accuracy and user computation and communication resources, and use the corresponding algorithm to solve them. Moreover, we also infer the condition for optimal transmission time, and through the iteration between algorithms to obtain the final converged solution. Through simulation verification, our proposed algorithm is compared with the fixed altitude UAV-assisted FL ratio, ensuring the learning performance and reducing the total energy consumption of users. Moreover, because the baseline algorithm FLA does not optimize local accuracy and the baseline algorithm FTT does not optimize transmission time, so the total system cost and total energy consumption of them are also higher than the proposed algorithm.

Of course, there are some improvements in this article, the UAV altitude in our paper is obtained through traversal and so perhaps there is a better way to optimize the UAV altitude. Moreover, in the future, this scenario may be extended to the scenario of multi-UAV-assisted FL.

Author Contributions: Conceptualization: C.L. and Q.Z.; methodology: C.L.; software: C.L.; validation: C.L. and Q.Z.; formal analysis: C.L.; investigation: C.L.; resources: Q.Z.; data curation: C.L.; writing: C.L.; visualization: C.L.; supervision: Q.Z.; project administration: Q.Z.; funding acquisition: Q.Z. All authors have read and agreed to the published version of the manuscript.

Funding: This work is supported by the National Natural Science Foundation of China (61971239, 92067201), Jiangsu Provincial Key Research and Development Program (No. BE2022068-2).

Institutional Review Board Statement: Not applicable.

Informed Consent Statement: Not applicable.

Data Availability Statement: Not applicable.

Conflicts of Interest: The authors declare no conflict of interest.

References

1. Zhou, Z.; Chen, X.; Li, E.; Zeng, L.; Luo, K.; Zhang, J. Edge Intelligence: Paving the Last Mile of Artificial Intelligence With Edge Computing. *Proc. IEEE* **2019**, *107*, 1738–1762. [CrossRef]
2. Li, T.; Sahu, A.K.; Talwalkar, A.; Smith, V. Federated Learning: Challenges, Methods, and Future Directions. *IEEE Signal Process. Mag.* **2020**, *37*, 50–60. [CrossRef]
3. Mcmahan, H.B.; Moore, E.; Ramage, D.; Hampson, S.; y Arcas, B.A. Communication-Efficient Learning of Deep Networks from Decentralized Data. In Proceedings of the International Conference on Artificial Intelligence and Statistics, Bangkok, Thailand, 24–25 January 2016. [CrossRef]
4. Nishio, T.; Yonetani, R. Client Selection for Federated Learning with Heterogeneous Resources in Mobile Edge. In Proceedings of the ICC 2019–2019 IEEE International Conference on Communications (ICC), Shanghai, China, 20–24 May 2019; pp. 1–7.
5. Yoshida, N.; Nishio, T.; Morikura, M.; Yamamoto, K. MAB-based Client Selection for Federated Learning with Uncertain Resources in Mobile Networks. In Proceedings of the 2020 IEEE Globecom Workshops, Taipei, Taiwan, 7–11 December 2020; pp. 1–6. [CrossRef]
6. Xu, B.; Xia, W.; Zhang, J.; Quek, T.Q.S.; Zhu, H. Online Client Scheduling for Fast Federated Learning. *IEEE Wirel. Commun. Lett.* **2021**, *10*, 1434–1438. [CrossRef]
7. Yang, H.H.; Arafa, A.; Quek, T.Q.S.; Poor, H.V. Age-Based Scheduling Policy for Federated Learning in Mobile Edge Networks. In Proceedings of the IEEE International Conference on Acoustics, Speech and Signal Processing, Barcelona, Spain, 4–8 May 2020; pp. 8743–8747. [CrossRef]
8. Ren, J.; He, Y.; Wen, D.; Yu, G.; Huang, K.; Guo, D. Scheduling for Cellular Federated Edge Learning With Importance and Channel Awareness. *IEEE Trans. Wirel. Commun.* **2020**, *19*, 7690–7703. [CrossRef]

9. Liu, Y.; Tian, M.; Chen, Y.; Xiong, Z.; Leung, C.; Miao, C. A Contract Theory based Incentive Mechanism for Federated Learning. In Proceedings of the International Work-shop on Federated and Transfer Learning for Data Sparsity and Confidentiality in Conjunction with IJCAI, Online, 12 August 2021. [CrossRef]
10. Yang, Z.; Chen, M.; Saad, W.; Hong, C.S.; Shikh-Bahaei, M. Energy Efficient Federated Learning Over Wireless Communication Networks. *IEEE Trans. Wirel. Commun.* **2020**, *20*, 1935–1949. [CrossRef]
11. Luo, S.; Chen, X.; Wu, Q.; Zhou, Z.; Yu, S. HFEL: Joint Edge Association and Resource Allocation for Cost-Efficient Hierarchical Federated Edge Learning. *IEEE Trans. Wirel. Commun.* **2020**, *19*, 6535–6548. [CrossRef]
12. Zeng, Q.; Du, Y.; Huang, K.; Leung, K.K. Energy-Efficient Resource Management for Federated Edge Learning With CPU-GPU Heterogeneous Computing. *IEEE Trans. Wirel. Commun.* **2021**, *20*, 7947–7962. [CrossRef]
13. Ruby, R.; Yang, H.; de Figueiredo, F.A.P.; Huynh-The, T.; Wu, K. Energy-Efficient Multi-Processor-based Computation and Communication Resource Allocation in Two-Tier Federated Learning Networks. *IEEE Internet Things J.* **2022**, *1*, 1. [CrossRef]
14. Le, T.H.T.; Tran, N.H.; Tun, Y.K.; Nguyen, M.N.H.; Pandey, S.R.; Han, Z.; Hong, C.S. An Incentive Mechanism for Federated Learning in Wireless Cellular Networks: An Auction Approach. *IEEE Trans. Wirel. Commun.* **2021**, *20*, 4874–4887. [CrossRef]
15. Chen, M.; Yang, Z.; Saad, W.; Yin, C.; Poor, H.V.; Cui, S. A Joint Learning and Communications Framework for Federated Learning Over Wireless Networks. *IEEE Trans. Wirel. Commun.* **2020**, *20*, 269–283. [CrossRef]
16. Wen, W.; Chen, Z.; Yang, H.H.; Xia, W.; Quek, T.Q.S. Joint Scheduling and Resource Allocation for Hierarchical Federated Edge Learning. *IEEE Trans. Wirel. Commun.* **2022**, *21*, 5857–5872. [CrossRef]
17. Liu, S.; Yu, G.; Chen, X.; Bennis, M. Joint User Association and Resource Allocation for Wireless Hierarchical Federated Learning With IID and Non-IID Data. *IEEE Trans. Wirel. Commun.* **2022**, *21*, 7852–7866. [CrossRef]
18. Shi, W.; Zhou, S.; Niu, Z.; Jiang, M.; Geng, L. Joint Device Scheduling and Resource Allocation for Latency Constrained Wireless Federated Learning. *IEEE Trans. Wirel. Commun.* **2020**, *20*, 453–467. [CrossRef]
19. Yang, K.; Jiang, T.; Shi, Y.; Ding, Z. Federated Learning via Over-the-Air Computation. *IEEE Trans. Wirel. Commun.* **2020**, *19*, 2022–2035. [CrossRef]
20. Al-Abiad, M.S.; Hassan, Z.; Hossain, J. Energy-Efficient Resource Allocation for Federated Learning in NOMA-Enabled and Relay-Assisted Internet of Things Networks. *IEEE Internet Things J.* **2022**, *9*, 24736–24753. [CrossRef]
21. Xiao, H.; Zhao, J.; Pei, Q.; Feng, J.; Liu, L.; Shi, W. Vehicle Selection and Resource Optimization for Federated Learning in Vehicular Edge Computing. *IEEE Trans. Intell. Transp. Syst.* **2021**, *23*, 11073–11087. [CrossRef]
22. Tursunboev, J.; Kang, Y.-S.; Huh, S.-B.; Lim, D.-W.; Kang, J.-M.; Jung, H. Hierarchical Federated Learning for Edge-Aided Unmanned Aerial Vehicle Networks. *Appl. Sci.* **2022**, *12*, 670. [CrossRef]
23. Pham, Q.-V.; Le, M.; Huynh-The, T.; Han, Z.; Hwang, W.-J. Energy-Efficient Federated Learning over UAV-Enabled Wireless Powered Communications. *IEEE Trans. Veh. Technol.* **2022**, *71*, 4977–4990. [CrossRef]
24. Ng, J.S.; Lim, W.Y.B.; Dai, H.-N.; Xiong, Z.; Huang, J.; Niyato, D.; Hua, X.-S.; Leung, C.; Miao, C. Joint Auction-Coalition Formation Framework for Communication-Efficient Federated Learning in UAV-Enabled Internet of Vehicles. *IEEE Trans. Intell. Transp. Syst.* **2020**, *22*, 2326–2344. [CrossRef]
25. Jing, Y.; Qu, Y.; Dong, C.; Shen, Y.; Wei, Z.; Wang, S. Joint UAV Location and Resource Allocation for Air-Ground Integrated Federated Learning. In Proceedings of the IEEE Global Communications Conference, Madrid, Spain, 7–11 December 2021; pp. 1–6. [CrossRef]
26. Yang, H.; Zhao, J.; Xiong, Z.; Lam, K.-Y.; Sun, S.; Xiao, L. Privacy-Preserving Federated Learning for UAV-Enabled Networks: Learning-Based Joint Scheduling and Resource Management. *IEEE J. Sel. Areas Commun.* **2021**, *39*, 3144–3159. [CrossRef]
27. Lyu, J.; Zeng, Y.; Zhang, R. UAV-Aided Offloading for Cellular Hotspot. *IEEE Trans. Wirel. Commun.* **2018**, *17*, 3988–4001. [CrossRef]
28. Dinkelbach, W. On nonlinear fractional programming. *Manag. Sci.* **1967**, *13*, 492–498. [CrossRef]

Disclaimer/Publisher's Note: The statements, opinions and data contained in all publications are solely those of the individual author(s) and contributor(s) and not of MDPI and/or the editor(s). MDPI and/or the editor(s) disclaim responsibility for any injury to people or property resulting from any ideas, methods, instructions or products referred to in the content.